Mapping of a Cellulose-Deficient Mutant Named *dwarf1-1* in *Sorghum bicolor* to the Green Revolution Gene *gibberellin20-oxidase* Reveals a Positive Regulatory Association between Gibberellin and Cellulose Biosynthesis[1][OPEN]

Carloalberto Petti, Ko Hirano, Jozsef Stork, and Seth DeBolt*

Department of Horticulture, University of Kentucky, Lexington, Kentucky 40546 (C.P., J.S., S.D.); and Bioscience and Biotechnology Center, Nagoya University, Nagoya 464–8601, Japan (K.H.)

ORCID IDs: 0000-0001-7521-3615 (C.P.); 0000-0002-5473-526X (J.S.).

Here, we show a mechanism for expansion regulation through mutations in the green revolution gene *gibberellin20* (*GA20*)-*oxidase* and show that GAs control biosynthesis of the plants main structural polymer cellulose. Within a 12,000 mutagenized *Sorghum bicolor* plant population, we identified a single cellulose-deficient and male gametophyte-dysfunctional mutant named *dwarf1-1* (*dwf1-1*). Through the *Sorghum propinquum* male/*dwf1-1* female F2 population, we mapped *dwf1-1* to a frameshift in *GA20-oxidase*. Assessment of GAs in *dwf1-1* revealed ablation of GA. GA ablation was antagonistic to the expression of three specific *cellulose synthase* genes resulting in cellulose deficiency and growth dwarfism, which were complemented by exogenous bioactive gibberellic acid application. Using quantitative polymerase chain reaction, we found that GA was positively regulating the expression of a subset of specific *cellulose synthase* genes. To cross reference data from our mapped *Sorghum* sp. allele with another monocotyledonous plant, a series of rice (*Oryza sativa*) mutants involved in GA biosynthesis and signaling were isolated, and these too displayed cellulose deficit. Taken together, data support a model whereby suppressed expansion in green revolution GA genes involves regulation of cellulose biosynthesis.

In all higher plants, development of upright plant growth is advanced by a highly regulated process of cell division, cell fate determination, and cell expansion (Xie et al., 2011). Cell shape and morphogenesis are largely acquired through anisotropic expansion, during which the plant cell wall provides the structural integrity needed to resist internal turgor pressure and simultaneously extend in a controlled and organized manner (Cosgrove and Jarvis, 2012). Cellulose is the main load-bearing component on the plant cell wall, and cellulose is synthesized in a highly organized manner according to the expansion state and growth pattern (Tsekos, 1999). A number of phytohormones are involved in regulating expansion, including auxin (Paque et al., 2014), brassinosteroid (Xie et al., 2011), the rapid alkalinization factor peptide hormone (Haruta et al., 2014), cytokinin (Downes and Crowell, 1998), and GAs (Keyes et al., 1989). A complex and still poorly understood interplay exists among phytohormones to precisely regulate cellular expansion machinery.

Sorghum bicolor is one of the most agriculturally important grains produced worldwide (Paterson, 2008). It is largely cultivated in Africa, India, China, and the United States for both grain and biomass. An advantage that *Sorghum* sp. holds over many other grain crops is drought tolerance, an important trait in low-rainfall conditions and anticipated climate change shifts (Schmidhuber and Tubiello, 2007). The *Sorghum* sp. genome (730 Mb; Paterson et al., 2009) is much smaller than maize (*Zea mays*; 2,500 Mb) and most grasses (e.g. wheat [*Triticum aestivum*], 15,000 Mb; barley [*Hordeum vulgare*], 5,100 Mb), and genetic tools are available (Paterson et al., 2009; Liu and Godwin, 2012). Here, we aimed to isolate a cellulose-deficient mutant from within a chemical mutagenesis population, which we named *dwarf1-1* (*dwf1-1*). From here, we aimed to characterize the genetic mutation underlying severe cellulose deficiency and aberrant expansion in a *dwf1-1*. Most cellulose-deficient mutants have been mapped to cellulose synthase (*CESA*) genes (Arioli et al., 1998; Taylor et al., 2003; Sethaphong et al., 2013).

[1] This work was supported by the Japan Society for the Promotion of Science (KAKENHI grant no. 26660278 to K.H.), the U.S. Department of Energy (grant no. Department of Energy-Funding Opportunity Announcement 10–0000368 to S.D.), and the National Science Foundation (grant nos. 1256029 and 1355438 to S.D.).

* Address correspondence to sdebo2@uky.edu.

The author responsible for distribution of materials integral to the findings presented in this article in accordance with the policy described in the Instructions for Authors (www.plantphysiol.org) is: Seth DeBolt (sdebo2@uky.edu).

C.P. performed most of the experiments with technical assistance from J.S. and K.H.; S.D. conceived the project and wrote the article with C.P.

[OPEN] Articles can be viewed without a subscription.
www.plantphysiol.org/cgi/doi/10.1104/pp.15.00928

dwf1-1 did not map to a *CESA* gene but rather, mapped to a *GA20-oxidase* involved in GA biosynthesis. We then sought to explore the feedback between dwarfism and cellulose deficiency and used rice (*Oryza sativa*), because many of the GA biosynthetic mutants are characterized as green revolution genes. Chemical inhibition, exogenous GA complementation, transcriptional analyses, and phenotypic data were used to support our findings.

RESULTS

dwf1-1 Displays Dwarfed Morphology and Reduced Cellulose Content

The *Sorghum* sp. *dwf1-1* mutant arose from an M2 mutagenesis population that we developed (as described in "Materials and Methods"). The mutant was immediately identifiable compared with the wild type because of a lack of expansion and extremely dwarfed morphology (Fig. 1, A and B). Expansion defects and dwarfed plant form persisted until reaching maturity (Fig. 1B). The mutant displayed a reduction in total plant height (Fig. 1C) equivalent to one-tenth the size of mature wild-type plants. Cellulose content was determined in M2 *dwf1-1* plants and found to be around 30% lower than that in the wild type. Leaf and stem cellulose content was measured and found to be significantly lower than that in the wild type in both phenological growth stages assessed (Fig. 1D; $P < 0.001$ and $P < 0.01$, Student's t test).

Infertile Pollen in *dwf1-1* and Inheritance Analysis Using Wild-Type Pollen

Inflorescence from *dwf1-1* was unable to produce seed. A plausible explanation was that severe cellulose-deficient mutants, such as Arabidopsis (*Arabidopsis thaliana*) *cesa1* and *Atcesa3*, were determined to be male

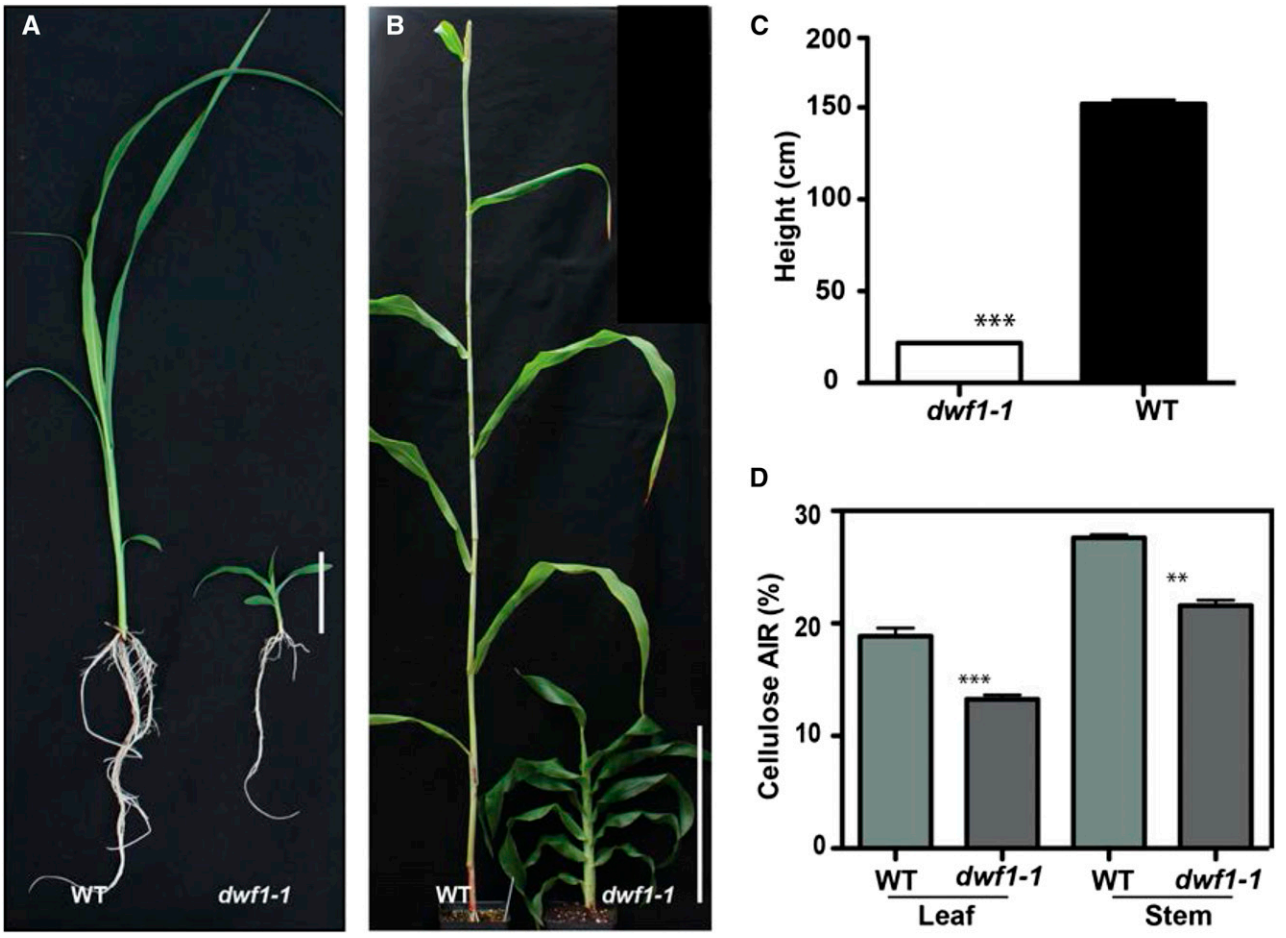

Figure 1. *dwf1-1* displays dwarfed plant form and cellulose deficit. A, Wild-type (WT) and *dwf1-1* plants grown in natural light conditions for 2 weeks in the greenhouse (24°C). Bar = 5 cm. B, The fully expanded mature wild type and *dwf1-1*. Bar = 25 cm. C, Height measurement between *dwf1-1* and the wild type evaluated at maturity ($n = 100$). D, Cellulose content was measured as a proportion of AIR and determined on leaves and stems of *dwf1-1* and the wild type ($n = 4$; error bars indicate SEM). Asterisks indicate significance by Student's t test. **, $P = 0.01$; ***, $P = 0.001$.

gametophytic lethal (Persson et al., 2007), and this may also be the case for *dwf1-1*. We therefore characterized pollen viability and germination (Fig. 2). It was found that the *dwf1-1* pollen did not germinate compared with robust germination in the wild type (Fig. 2, D–F). Germination in the wild type was approximately 45%, and this rate is in agreement with previous reports indicating the germination rates in *Sorghum* sp. (Lansac et al., 1994; Tuinstra and Wedel, 2000; Burke et al., 2007). Additional histochemical staining with aniline blue, 4′,6-diamidino-2-phenylindole, and Fluorescein Diacetate also showed differences in the health of *dwf1-1* pollen. Approximately one-half of the *dwf1-1* pollen grains were found to be nonviable according to a modified Alexander stain method (Peterson et al., 2010; Fig. 2, A–C). To test for female gametophyte fertility, we crossed wild-type pollen onto the stigma of *dwf1-1*, and the resulting cross was fertile and capable of producing viable seed.

For trait inheritance analysis, pollen from the wild type was used and crossed into *dwf1-1*. Because the mutant arose from the M2, we anticipated it to be a recessive trait. This was quantitatively verified in the F2 *dwf1-1* and wild-type cross. Here, 440 seedlings were assessed, and it was determined that 346 were phenotypically equivalent to the wild type and that 94 were *dwf1-1*, which was statistically a 3:1 ratio (χ^2 = 1.634, degrees of freedom = 1, $P > 0.05$). Additional populations were analyzed, and they verified a consistent 3:1 inheritance of the trait. Thus, we observed *dwf1-1* inheritance that was consistent with a single recessive gene inherited in a Mendelian manner.

The *dwf1-1* Mutation Maps to a *GA20-oxidase* and Not to a *CESA* Gene

The parental lines used for map-based cloning were *dwf1-1* (parent 1) as the female receptor and wild-type species *Sorghum propinquum* (parent 2) as the pollen donor, and the segregating population in the F2 generation was assessed. Genetic markers for *S. bicolor* × *S. propinquum* were derived from the works by Bhattramakki et al. (2000) and Billot et al. (2013). Bulked segregant analysis allowed for a linkage of *dwf1-1* to the lower arm of chromosome 10. Additional markers from chromosome 10 were obtained (Xu et al., 1995; Bhattramakki et al., 2000; Kong et al., 2000, 2013; Menz et al., 2002; Billot et al., 2013), and we determined that the mutation was associated to a region approximately 8-cm long between the genome landmark of Xtxp141 and Xcup3 (Fig. 3, A and B). Selected Cleaved Amplified Polymorphic Sequences (CAPS) markers and chromosome walking linked the mutation to a group of *GA20-oxidase*s. Cloning and sequencing (all primers in Supplemental Table S1) of the *GA20-oxidase* identified a frameshift mutation, which caused the loss of 60 amino acids within the first splice variant and 40 amino acids in

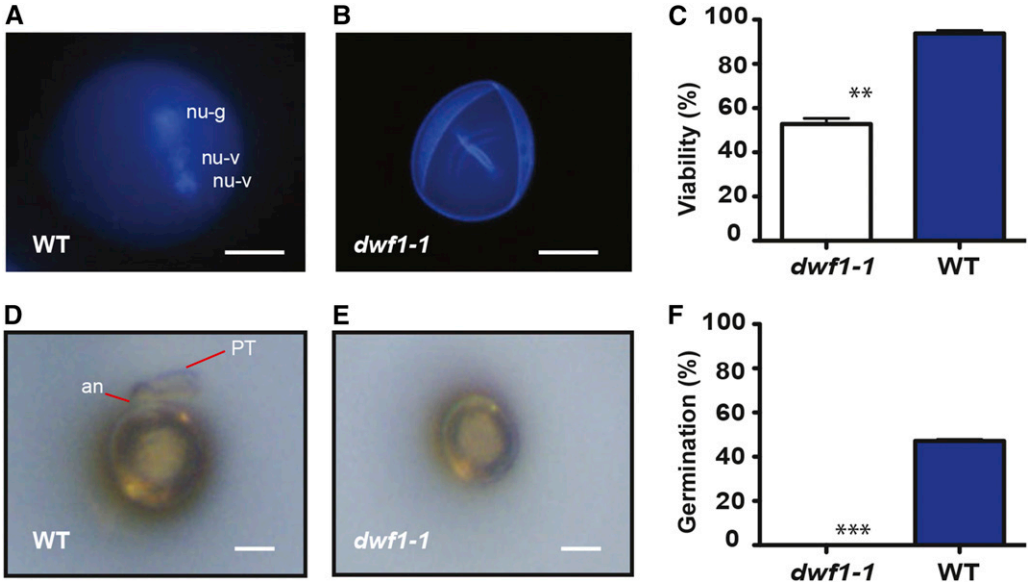

Figure 2. Pollen viability and germination are dysfunctional in *dwf1-1*. A, Example of wild-type (WT) pollen that has been stained with 4′,6-diamidino-phenylindole to show the three-nucleated pollen grain and spherical shape. nu-g, Germinative nuclei; nu-v, vegetative nuclei. Bar = 10 μm. B, Representative example of *dwf1-1* pollen highlighting internally collapsed surface, absence of nuclei, and aberrant spherical shape. Bar = 10 μm. C, Viability of pollen grains determined by a modified Alexander stain (n = 100; error bar is SEM of three technical replicates). Asterisks indicate significance by Student's t test. **, P = 0.01. Light micrographs of pollen germination determined in the wild type (D) and *dwf1-1* (E). In the wild type, evidence of the protruding annulus (an) and the germinating pollen tube (PT) is noted, but they are absent in *dwf1-1*. Bar = 10 μm. F, Germination rate determined as the percentage of pollen that developed the pollen tube (error bars represent SEM; n = 3 independent replications [100 counts each]). Asterisks indicate significant difference. ***, P = 0.001.

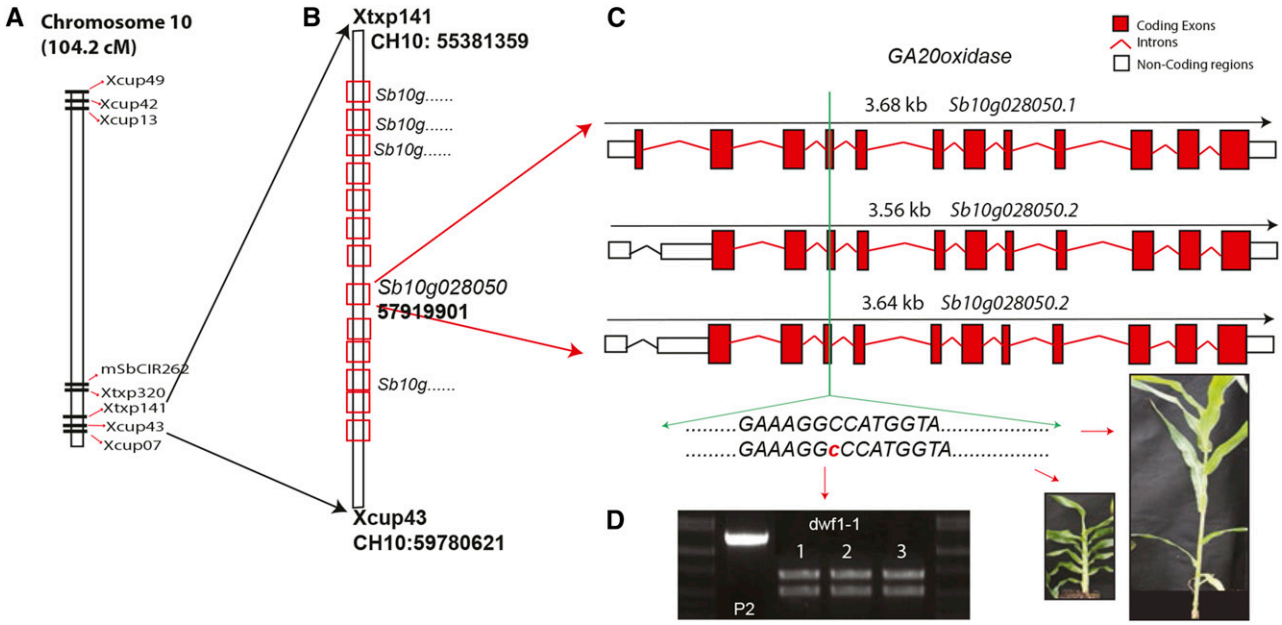

Figure 3. Map-based cloning of *dwf1-1*. A, Physical map of chromosome 10 with relevant SSR markers (Kong et al., 2013). B, Genomic region between SSR markers Xtxp141 and Xcup43 with the location of the genetic locus for the *GA20-oxidase* (*Sb10g028050*). C, The three alternative gene models (splice variant) determined for *Sb10g028050* with the position of the frameshift mutation highlighted. D, CAPS marker for the area containing the mutation observed in the *dwf1-1* population (examples 1–3) but not in wild-type *S. propinquum* (P2; plant specimen indicated by red arrows).

the remaining two alternative splicing forms of the gene (Fig. 3C; *Sb10g28050*). CAPS marker within the region containing the mutation verified the mapping population, with all but the parental *S. propinquum* containing the mutation (Fig. 3D).

Undetectable Levels of GAs in *dwf1-1*

A metabolic investigation of plant hormones was performed (Plant Hormone Analysis Laboratory; National Research Council of Canada). Numerous GAs were present in wild-type tissue, including GA3, GA7, GA19, GA20, GA24, GA44, and GA53 (Fig. 4). By contrast, no detectable GAs were measured in *dwf1-1* (Fig. 4). These data implied that the early 13 hydroxylation pathway conducive to formation of bioactive GA1 and GA8 (not bioactive GA; GA53 → GA44 → GA19 → GA20 → GA29 → GA1 → GA8) was dysfunctional in *dwf1-1*. In the assessment of hormones (Plant Hormone Analysis Laboratory; National Research Council of Canada), GA12 was not included, and GA53 was detected at 4 ng g^{-1} dry weight of wild-type tissue, which was not represented graphically (Fig. 4). The absence of any significant levels of GAs in the *dwf1-1* was consistent with a metabolic block in the biosynthetic pathway and the genetic dysfunction

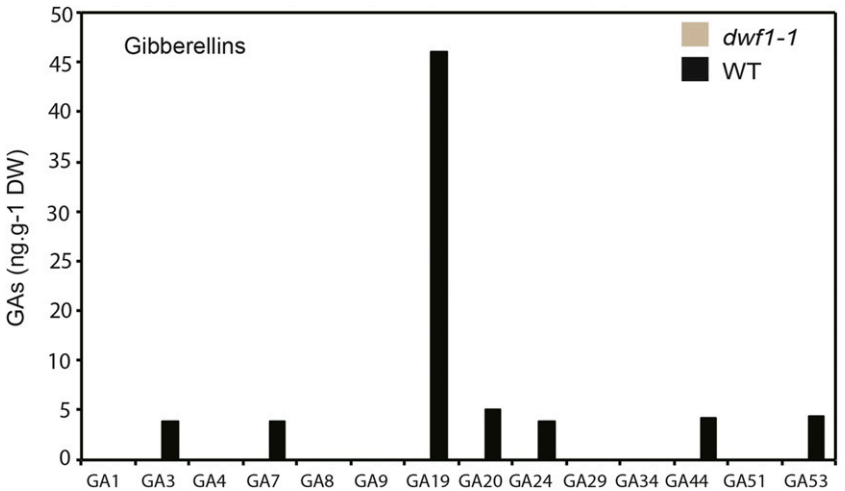

Figure 4. Analyses of GAs. *dwf1-1* and the wild type grown were examined for the occurrence of 12 key metabolic GAs. No GAs were detected in the *dwf1-1*, whereas the main GAs in the 13 early hydroxylation pathway were quantified for the wild type (WT). DW, Dry weight.

in the GA pathway. Additionally, sampling time may have been important to reveal the abundance of different GAs. For example, in our analysis, we did not detect GA1, GA4, or GA8, but the precursors were evident in wild-type tissue: GA19 to GA20 to GA4 to GA1. GAs are highly regulated by light and photoperiodism, and a prior study (Lee et al., 1998) showed that the highest level of GA53 corresponds to the lowest levels of GA1 and GA8. It was, therefore, plausible that our sampling focused on a proportionally high point in production of GA53 and GA19, which correspondingly overlapped with a low sampling point for GA1 and GA8. Importantly, transcriptional analysis of early genes in GA biosynthesis (stages 1 and 2; Hedden and Kamiya, 1997; Hedden and Phillips, 2000) revealed a lack of differential expression (Supplemental Fig. S1). These data were consistent with the downstream position of *GA20-oxidase* in the GA pathway. Other hormones analyzed (auxins and cytokinins) failed to display notable differences in accumulation (Supplemental Fig. S2). Taken together, data were consistent with a nonredundant role for the *GA20-oxidase* encoded by *dwf1-1* in biosynthesis of GA.

dwf1-1 Phenotype Is Rescued by the Application of Exogenous GA_3

In prior studies, phenotypes linked to GA deficit could be complemented with exogenous GA (Hedden and Phillips, 2000). Furthermore, recent chemical complementation experiments of GA mutants in *Sorghum* sp. used application of exogenous GA_3 (Ordonio et al., 2014), consistent with the work by Lee et al. (1998). Therefore, we hypothesized that the genetic block leading to no bioactive GAs in *dwf1-1* could be chemically complemented by application of exogenous GA_3. Importantly, this was a two-tiered question to establish whether either or both (1) cellulose deficiency and (2) dwarf phenotype could be complemented using GA_3 applied to *dwf1-1*. Because of male gametophytic lethality, the homozygous *dwf1-1* seedlings were selected from a segregating F2 population. Upon transplanting homozygous *dwf1-1* to GA_3-supplemented media, the dwarfed growth phenotype was fully rescued (Fig. 5, A and B). On a timescale, within 2 d of GA_3 application, the *dwf1-1* (height) grew 60% in length compared with the *dwf1-1*-control. Wild-type plants also reached a greater height (7.6% increase) compared with the untreated wild-type control. After 5 d of exposure, wild-type plants exposed to GA_3 displayed a 12% increase compared with untreated controls. However, the *dwf1-1* was 120% longer than *dwf1-1* controls after 5 d and phenotypically indistinguishable from the wild type. These data support chemical complementation of the *dwf1-1* by GA_3, which is in agreement with the lack of GAs. Also, cellulose deficit in *dwf1-1* was rescued with exogenous GA_3. Here, after 7 d exposure to 5 μM GA_3, the cellulose

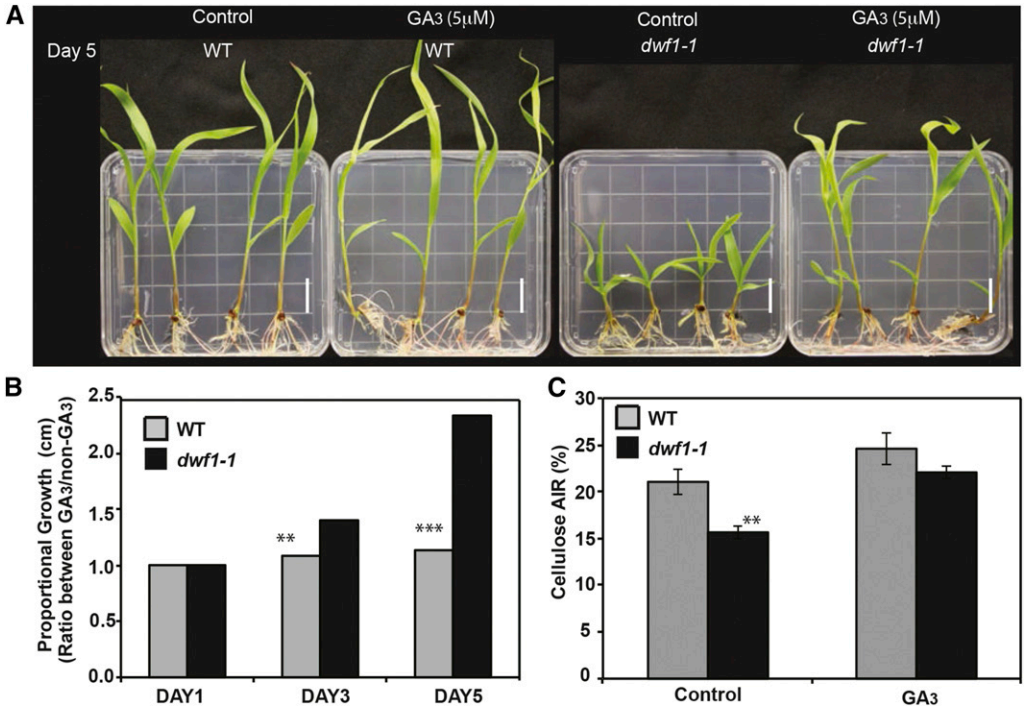

Figure 5. Chemical complementation of *dwf1-1*. A, Visual assessment of *dwf1-1* and the wild type (WT) grown for 5 d in media supplemented with exogenous GA_3. Bar = 1 cm. B, Proportional growth observed on the GA_3- versus the non-GA_3-treated wild type and *dwf1-1*. Proportions are presented. Statistical assessment was performed on expansion capacity of aerial plant tissue with $n = 4$ with five technical replicates. C, Bars indicate cellulose content (as a proportion of AIR). Control is untreated compared with the GA_3-treated wild-type and *dwf1-1* samples ($n = 4$ with five technical replicates; error bars represent SEM). Asterisks indicate significance by Student's *t* test. **, $P = 0.01$; ***, $P = 0.001$.

content in *dwf1-1* was almost identical to that in the wild type, and although marginally lower, it was found not to be significantly different ($P = 0.1246$, Student's t test; Fig. 5C). Thus, cellulose and dwarfism phenotypes in *dwf1-1* were linked to a GA deficit as expected from the genetic linkage data.

In addition to dwarfism and cellulose deficiency, the *dwf1-1* line was characterized by male sterility. Therefore, we sought to determine if the application of GA_3 could revert male infertility. After GA_3 application, it was found that the inflorescences were able to set seeds, albeit in a small percentage (5%–10%). The plantlets arising from seeds were phenotypically equivalent to the maternal *dwf1-1* line.

GA Inhibition Reduces Cellulose Synthesis in the Wild Type But Not in *dwf1-1*

By theory, pharmacological inhibition of GA biosynthesis should phenocopy genetic dysfunction with respect to causing reduced cellulose synthesis. This experiment was also important to pharmacologically mimic the *dwf1-1* mutant. To test this, after plants were sufficiently past seedling emergence stage and the first true leaves began to expand, they were transplanted to media supplemented with 0.2 or 0.4 mM chlorocholine chloride (CCC) and 0.2 or 0.4 mM daminozide (DMZ), both inhibitors of GA biosynthesis. In the wild type, a substantial drop in cellulose was observed after inhibition of GA (Fig. 6; $P = 0.001$), consistent with the genetic data earlier presented. By contrast, in the *dwf1-1* mutant background, there was no significant change in the cellulose content after pharmacological inhibition of GA (Fig. 6). Therefore, GA regulation, both genetically and pharmacologically, may account for a significant capacity of cellulose biosynthesis in *Sorghum* sp.

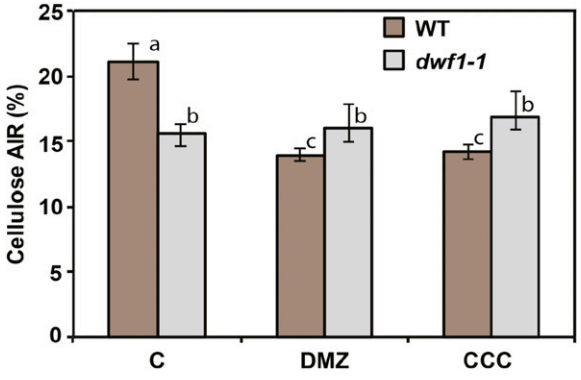

Figure 6. Pharmacological inhibition of GA causes cellulose deficit. The result of applying two different GA inhibitors (DMZ and CCC) was assessed compared with untreated controls (C). Cellulose content was measured as the proportion of AIR in wild-type (WT) and *dwf1-1* plantlets (aerial tissue) after 10 d of exposure compared with C. ANOVA was used to established significance between and across groups ($n = 4$ with five technical replicates). Different letters indicate significance established at $P \leq 0.05$.

However, our observations do not exclude contributions to cellulose regulation from other mechanisms.

Rice GA Mutants Phenocopy *Sorghum* sp. *dwf1-1* in Cellulose Deficiency

In lieu of our map-based cloning of a single mutant allele identified from within our 12,000 *Sorghum* sp. population and the difficulties in transformation of the parental sweet *Sorghum* sp. variety for single-gene complementation, we sought to identify alleles in another monocotyledonous species: rice. To evaluate how GA dysfunction impacted cellulose biosynthesis, six GA-related mutant lines with semidwarf or dwarf phenotypes were examined (Fig. 7). Two groups of semidwarf mutants defective in GA biosynthesis were investigated. Mutant alleles of *semidwarf-1* (*sd-1*; *ga20-oxidase*), including two *sd-1* intermediate alleles (sc^{Reimei} and $sc^{Shiranui}$) and one *sd-1* null allele (sc^{TN-1}; Xia et al., 1991; Ogi et al., 1993; Irie et al., 2008), were grown alongside and compared with their parent wild-type Norin 29 (Fig. 7). Here, sc^{Reimei} is the weakest allele, and sc^{TN-1} is the most severe (Okuno et al., 2014). Corresponding, mutations all induced a reduction in cellulose biosynthesis (milligrams per gram cell wall acid-insoluble residue [AIR]).

To further explore the link between GA and cellulose biosynthesis, we examined cellulose content in a mild mutation in ent-kaurene oxidase (KO; *Tan-Ginbozu*), which catalyzed an early step in GA biosynthesis (Itoh et al., 2004; Okuno et al., 2014) compared with its parental *Ginbozu*. This class of mutation in the GA biosynthetic pathway also resulted in less cellulose content (milligrams per gram AIR) than that in parental plants (Fig. 7).

We questioned whether dysfunctional GA signaling may also cause reduced cellulose content. Therefore, we examined mutations in *SLENDER1* (*SLR1*) and *GIBBERELLIN INSENSITIVE DWARF1* (*GID1*). *SLR1-d1* is a mutant encoding a constitutively active form of a suppressor protein for GA signaling: SLR1 (Ueguchi-Tanaka et al., 2007; Asano et al., 2009). By contrast, *GID1* encodes a soluble GA receptor that positively regulates GA signaling (Ueguchi-Tanaka et al., 2007), and thus, the above two mutants both show suppressed GA signaling. Interestingly, the reduction in cellulose content was modest and relatively consistent for GA signaling mutants compared with more severe GA biosynthetic mutants (Fig. 7).

Specific *CESA* Transcripts Were Down-Regulated in *dwf1-1* Mutant and Conversely Activated by Exogenous GA Application, Suggesting Regulatory Specificity

CESA genes were bioinformatically annotated based on prior phylogenetic studies that included Arabidopsis, setaria (*Setaria viridis*), and maize along with *Sorghum* sp. (Petti et al., 2013). Based on bioinformatic data available, we annotated a total of eight *Sorghum* sp. genes as *CESA*; they were Sb09g005280, Sb03g004310, Sb01g004210, Sb02g006290, Sb02g007810, Sb01g019720, Sb02g025020,

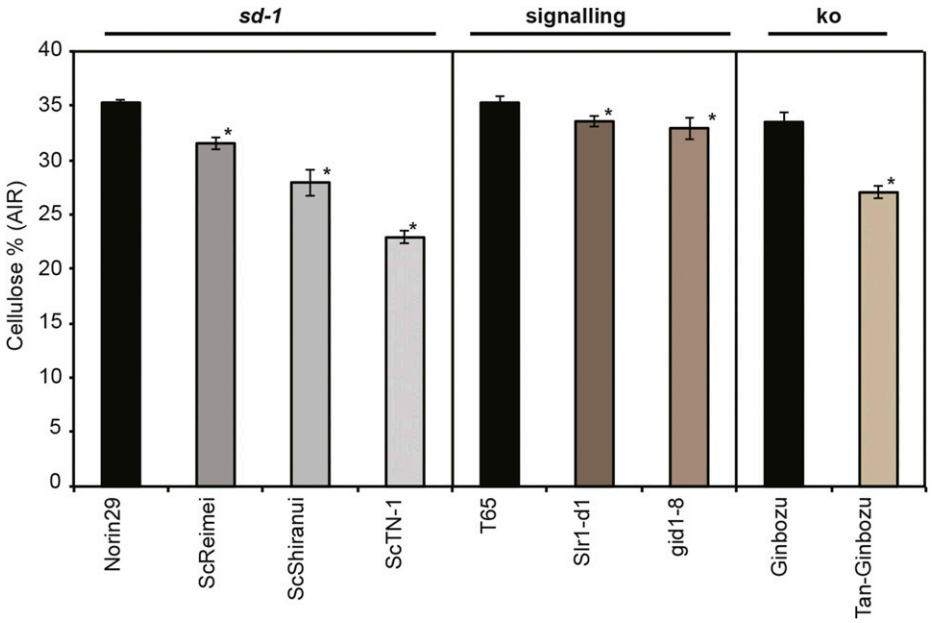

Figure 7. Analysis of cellulose biosynthesis in rice semidwarf varieties with GA dysfunction. The cellulose content of AIR from rice seedlings with genetic mutations in the GA pathway was determined on 10-d-old seedlings (10 d postgermination). For cellulose analysis, three composite biological replicates consisting of five seedlings each were used along with three technical replicates. Error bars indicate SEM of three replicates. *, Significance (P = 0.01) using a Student's t test from the mean of the appropriate control.

and Sb02g010110. Little is known about specific properties of the CESA complex in *Sorghum* sp., but by contrast, we know that primary and secondary cell wall CESA complexes acquire a heterotrimeric configuration in Arabidopsis (Desprez et al., 2007; Persson et al., 2007) with a probable stoichiometry of 1:1:1 (Gonneau et al., 2014), which displays coexpression at the transcriptional level (Brown et al., 2005; Persson et al., 2005). Although we cannot safely overlay data from the Arabidopsis system on monocotyledons because of notable differences in vascular development and physiological adaptations, we examined homology to functionally characterized *CESA* from Arabidopsis with the *Sorghum* sp. accessions. Results were Sb09g005280 (*CESA1-like* or *CESA10-like*), Sb03g004310 (*CESA1-like* or *CESA10-like*), Sb01g004210 (*CESA3-like*), Sb02g006290 (*CESA3-like*), Sb02g007810 (*CESA6-like*), Sb01g019720 (*CESA4-like*), Sb02g025020 (*CESA7-like*), and Sb02g010110 (*CESA81-like*). For our study, we sought to ask whether any differential expression occurred in *dwf1-1*. The transcripts that we annotated as primary cell wall-related Sb09g005280 (*CESA1-like* or *CESA10-like*), Sb01g004210 (*CESA3-like*), and Sb02g007810 (*CESA6-like*) were differentially down-regulated in a similar manner (Fig. 8; $P <$ 0.001). All other genes were not differentially expressed. These included putative *CESA* genes annotated as most homologous to the Arabidopsis cluster of three secondary cell wall CESA genes (*CESA4*, *CESA7*, and *CESA8*; $P > 0.05$; Fig. 8). Although this does not rule out GA-mediated regulation of secondary cell wall *CESA*s, it does illustrate a clustering of putative *CESA* genes that were down-regulated in the GA-deficient *dwf1-1*. To query transcriptional regulatory features, we examined the promoter region (4,000 bp upstream) of all *CESA* genes for the presence of cis-trans acting elements, particularly those related to hormone response in prior studies. The promoters of both primary and secondary *CESA* genes contained putative GA-, cytokinin-, and auxin-responsive elements (Supplemental Table S2). No clear pattern was evident, suggesting that additional work will be needed to decipher the transcriptional regulatory machinery involved.

To advance the question of whether GA was capable of positively regulating *CESA* transcription, we quantified transcript abundance for the *CESA* genes that were differentially down-regulated in *dwf1-1* in wild-type *Sorghum* sp. after the addition of exogenous bioactive GA_3. The experiment was performed by exogenously applying GA_3 to 10-d-old light-grown (16-h-light/8-h-dark cycle) *Sorghum* sp. seedlings for 1 h. Normalized against wild-type expression, the addition of GA_3 caused modest but significant increased gene expression for all three putative *CESA* genes (Fig. 9). In the *dwf1-1* mutant,

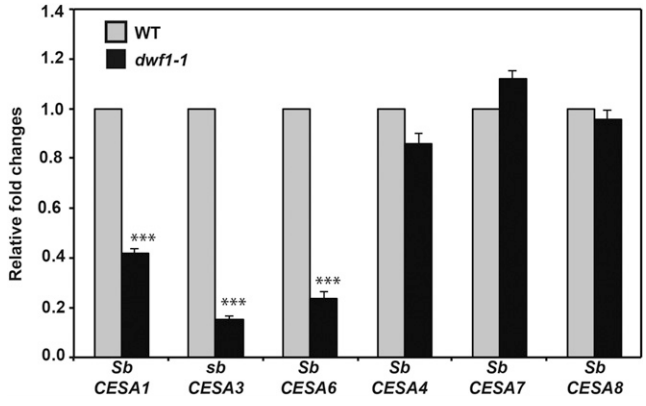

Figure 8. Transcriptional analysis of *Sorghum* sp. *CESA*s. The relative expressions of primary and secondary cell wall *SbCESA* genes (Petti et al., 2013) were determined by quantitative reverse transcription-PCR in 14-d-old plantlets (aerial tissue) from the wild type (WT) and *dwf1-1*. Error bars indicate SEM of three replicates. ***, Significance (P = 0.001).

we also examined gene expression before and after the addition of GA_3. In contrast with data from wild-type plants, the expression of *CESA* genes in *dwf1-1* was highly increased (5-fold) after GA_3 addition (Fig. 9).

DISCUSSION

Our forward genetics screen was in *Sorghum* sp. because of prior genetic screens for altered cellulose being performed in Arabidopsis. There are prominent differences between dicot and monocot cell walls. Arabidopsis has a type I cell wall, whereas most economically important biomass and grain crops are grasses with divergent type II cell walls (Carpita and Gibeaut, 1993). Our primary screen was for (1) dwarfed plant form and (2) cellulose deficit, which revealed *dwf1-1*. Map-based cloning of *dwf1-1* to *SbGA20-oxidase* was in contrast to both our expectations. Certainly, dwarfed and fertility-compromised mutant phenotypes were highly consistent with GA mutants, such as *ga1-3* (Cheng et al., 2004) and *gid1* (Aya et al., 2009) and also, show similar growth defects in rice (Sasaki et al., 2002) and Arabidopsis (Plackett et al., 2012) *GA20-oxidase* mutants. In fact, the rice *GA20-oxidase* mutant was isolated as a green revolution locus (Sasaki et al., 2002). However, current studies have mapped cellulose-deficient mutants to only a handful of genes, and most of these are *CESA*s (Arioli et al., 1998; Fagard et al., 2000; Desprez et al., 2002; Daras et al., 2009) or a small handful of CESA accessory proteins, including POM2/*CELLULOSE SYNTHASE INTERACTING1* (Lei et al., 2012), COBRA (Roudier et al., 2005), and KORRIGAN (Lane et al., 2001). With a genetic screen for cellulose deficit linked to *GA20-oxidase*, we uncovered a GA-mediated mechanism for regulating cellular expansion. Importantly, this result was supported by pharmacological inhibition of GA, which also led to cellulose deficit (Fig. 6). Correspondingly, in both wild-type parental lines and the *dwf1-1* mutant *CESA*, transcript abundance was significantly greater after exogenous GA_3 addition (Fig. 9), suggesting positive regulation. Thus, an obvious question from these results is whether cellulose deficit could be the feature of GA deficit that leads to poor pollen viability and dwarfed growth form. Several logical points are consistent with this possibility. Both *Atcesa1* and *Atcesa3* mutants are pollen lethal and severely dwarfed (Persson et al., 2007) as is *dwf1-1*. Dwarfed growth is a common feature of cellulose deficiency (Fagard et al., 2000; Desprez et al., 2002) and GA deficit (Koornneef and van der Veen, 1980). Furthermore, transcriptional feedback was observed between GA deficit in *dwf1-1* and primary cell wall *CESA*s (Fig. 7), which are known to be coregulated (Brown et al., 2005; Persson et al., 2005).

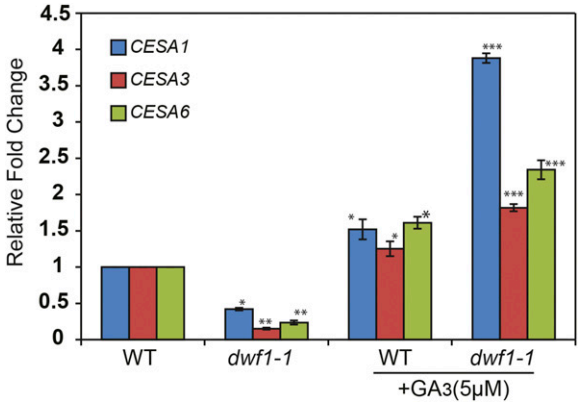

Figure 9. Transcriptional analysis of *Sorghum* sp. *CESA*s after GA application. The relative expressions of primary cell wall *SbCESA* genes were determined by quantitative reverse transcription-PCR in 7- to 10-d-old plantlets (aerial tissue) from the wild type (WT) and *dwf1-1* with and without GA_3 addition. Error bars indicate SEM of three replicates. Asterisks indicate significant difference. *, $P = 0.05$; **, $P = 0.01$; ***, $P = 0001$.

Primary and secondary cell wall cellulose biosyntheses have quite different roles in plant development. Transcriptional control of secondary cell wall *CESA*s has been studied, and several members of the NAC (for *NAM* [No Apical Meristem], *ATAF1-2*, and *CUC2* [Cup-Shaped Cotyledon]) family of transcription factors have been identified as key regulators (Yamaguchi et al., 2010). In primary cell wall cellulose synthesis, posttranscriptional (Held et al., 2008) and posttranslational control (Chen et al., 2010) features have been observed. Our results support the role of GA as a positive regulator of *CESA* initiated transcriptionally. However, an additional question is how other hormones needed for expansion fit with proposed GA regulation of cellulose biosynthesis. For example, auxin and brassinosteroid are also critical for controlled expansion (Frigerio et al., 2006; Xie et al., 2011; Wolf et al., 2012; Paque et al., 2014). Prior evidence suggests cross talk between auxin and GA metabolism in Arabidopsis to regulate expansion (Frigerio et al., 2006), which in some circumstance, can involve auxin signaling upstream of the GA (Paque et al., 2014). Furthermore, dysfunction in brassinosteroid levels also seems to influence both primary and secondary cell wall cellulose biosyntheses. This signal either exists divergent of GA as a developmentally or environmentally induced signal or interacts with GA. Deciphering such a regulatory signaling pattern will be important for our understanding of anisotropic expansion in plants. GA responsive elements (Chen et al., 2006) were identified within the promoter of *Sorghum* sp. *CESA* genes, suggesting the possibility for direct regulatory features. During review of this article, Huang et al. (2015) published a causal association between GA signaling and the secondary cellulose biosynthetic process in rice. Huang et al. (2015) propose a model whereby GA-mediated DELLA-NAC (SLR1) signaling of an MYB transcription factor directly regulates CESA transcription, which is consistent with prior studies (Yamaguchi et al., 2010). Huang et al. (2015) also illustrate a vehicle for possible interaction with auxin-mediated development (Frigerio et al., 2006; Paque et al., 2014), which is where SLR1 (NAC) has been previously characterized in Arabidopsis lateral root formation (Fukaki et al., 2002). It will be interesting to examine whether the

rice pathway is conserved in Arabidopsis and other species and how GA responses intersect with other hormonal signals during the regulation of plant expansion.

Classically involved in stem elongation, a mechanism for expansion regulation through GA involves antagonistic signaling between light and GAs (de Lucas et al., 2008). Interestingly, recent evidence suggests that *PHYTOCHROME INTERACTING FACTOR4* (*PIF4*) influences the cellulose biosynthetic process (Bischoff et al., 2011) in Arabidopsis. *PIF4* positively regulates genes involved in cellular expansion, and this is negatively regulated by the light photoreceptor phytochrome B (Huq and Quail, 2002). The transcriptional activity of *PIF4* is also blocked during light signaling by DELLA that binds to the recognition sites for target genes (de Lucas et al., 2008). Taken with the findings by Huang et al. (2015), here, the switch to photomorphogenesis upon exposure to light inhibits hypocotyl expansion through *PIF4*. Understanding whether interplay exists between GA-mediated photomorphogenesis and the regulation of the DELLA-NAC transcriptional machinery (Huang et al., 2015) will be interesting future work.

Because cellulose was significantly reduced but not ablated in *dwf1-1*, the possibility exists that GA regulation provides a necessary biosynthetic cue to maximize cellulose production during cell wall development. We postulate that high-density organization of cellulose and a requirement for biosynthesis during key times of cellular expansion likely need regulatory mechanism(s) to adequately allocate resources. GA seems to directly fulfill one such role in regulating cellulose biosynthetic processes in *Sorghum* sp. and rice.

MATERIALS AND METHODS

Generating Ethyl Methanesulfonate Mutagenesis Population in *Sorghum* sp.

Ethyl methanesulfonate (EMS; Sigma) causes preferential alkylation of guanidine and thus, a shift of G:C base paring to A:T and was used to generate an mutagenesis population in *Sorghum bicolor* (the parental wild type). Approximately 12,000 seeds were exposed to a lethality-based saturation assay to establish the required dose of EMS needed (0.25%–1.5% [w/v] with a stepwise increase of 0.25% [w/v]), the optimal EMS concentration being estimated as 0.75% (w/v). Seeds were then exposed to 0.75% (w/v) EMS for 12 h followed by neutralization in sodium thiosulfate (0.2 M) and sequentially washed (M0 generation). They were air dried and sown on soilless media (MetroMix 360; SunGro Industries) supplemented with 3 g of Osmocote (The Scotts Company) at field water conditions. Seedlings were grown in a temperature-controlled greenhouse before being transplanted to the field after 6 weeks. Plants were phenotypically scored for the occurrence of aberrant expansion and reduced cellulose content. One such line named *dwf1-1* was identified. For height estimation, 100 plants that were greenhouse grown were used for the mutant and the wild type. Plants of interest had their inflorescence bagged upon emergence to promote self-pollination. When this failed in the case of *dwf1-1*, the reciprocal cross between the wild type and *dwf1-1* was performed. Viable progeny and inheritance of the trait were ultimately established using pollen from the wild type and *dwf1-1* as the pollen receptor. The F2 population resulting from this cross was analyzed for the inheritance of the *dwf1-1* trait.

Additional Plant Material

For the rice (*Oryza sativa*) *sd-1* mutants, three isogenic lines (two intermediate alleles [sc^{Reimei} and $sc^{Shiranui}$] and one null allele [sc^{TN-1}]) were used with their recurrent parent, Norin 29 (Xia et al., 1991; Ogi et al., 1993; Irie et al., 2008). For the rice KO mutant, *Tan-Ginbozu* was used with its original cv Ginbozu (Itoh et al., 2004). For the rice GA-signaling mutants, *gid1-8* and *Slr1-d1* were used with their original cv Taichung 65 (Ueguchi-Tanaka et al., 2007; Asano et al., 2009). Briefly, seeds of each rice variety were surface sterilized and planted on one-half-strength Murashige and Skoog medium agar plates with and without GA_3 (5 μM) supplementation. Seeds were germinated and grown in a vertical position in an environmentally controlled growth chamber at 24°C with a 16-h-light/8-h-dark cycle. Biomass from the first internodes was used for the analysis of cellulose content of GA-deficient mutant rice varieties along with the respective wild-type controls. For cellulose analysis (described below), three composite biological replicates consisting of five seedlings each were used along with three technical replicates. Total seedling lengths were recorded for areal tissue 10 d postgermination.

Cellulose Quantification

Cell walls were prepared according to the work by Reiter et al. (1993), and cellulose estimation was completed on 5 mg of sample according to the work by Updegraff (1969). To standardize the comparison, tissue was staged (Petti et al., 2013) and used for biological and technical replicates. Whole stems were used, and leaves of identical position and age were collected from the mutant and the wild type.

Pollen Viability and Germination Test

Viability of the pollen grains for both the mutant and the wild type was tested according to the work by Peterson et al. (2010) in triplicate and at different times to account for the intrinsic variability of pollen viability (Lansac et al., 1994; Tuinstra and Wedel, 2000; Burke et al., 2007). Pollen and germinability of the *dwf1-1* and wild-type pollen were tested according to the works by Lansac et al. (1994) and Tuinstra and Wedel (2000) (n = 3; 100 counts each).

Mapping of the *dwf1-1* Mutant

Bulked segregant analysis was used to determine the mutation underlying the dwarf phenotype. The parental lines used were *dwf1-1* (parent 1) as the female receptor and the wild-type species *Sorghum propinquum* (parent 2) as the pollen donor. Genetic markers used were simple sequence repeats (SSRs) characterized and described for a similar cross type (*S. bicolor* × *S. propinquum*) in the works by Bhattramakki et al. (2000) and Billot et al. (2013). SSRs were tested for polymorphism in the parental lines P1 and P2 and a heterozygous F1. The SSRs displaying polymorphism were used for the analysis of the two bulks comprised of 25 individuals in each bulk. Equal amounts of purified DNA (4 μg) were used to generate the bulked DNA, and the final concentration used for the PCR analysis was 50 ng μL^{-1}. PCR products were visualized on a 3.5% (w/v) agarose gel and scored as P1, P2, or heterozygous. After chromosomal linkage, SSRs from published resources (Bhattramakki et al., 2000; Kong et al., 2000, 2013; Billot et al., 2013) and CAPS markers were developed to obtain a close association to a genetic marker on a population of 200 segregants of *dwf1-1*. Chromosome walking was used to identify targets genes, which were then PCR amplified and sequenced. Sequences were compared with the reference *S. bicolor* genomes sequence (Paterson et al., 2009) and *S. propinquum* (Mace et al., 2013).

Hormone Analysis

GAs (GA1, GA3, GA7, GA8, GA19, GA20, GA24, GA29, GA34, GA44, GA51, and GA53), auxin, and cytokinins were examined as described in the works by Abrams et al. (2003), Ross et al. (2004), and Zaharia et al. (2005). These analyses were commercially determined as a fee for service product by the National Research Council of Canada. Arial tissue samples for both *dwf1-1* and the wild type were light-grown 10-d-old seedlings.

Chemicals and Calibration Curves

A number of compounds, namely dihydroxyphaseic acid, abscisic acid (ABA)-glycosyl ester (GE), phaseic acid (PA), 7′- OH-ABA, neoPA, trans-ABA, and indole-3-acetic acid (IAA)-Glu, were synthesized and prepared at the National Research Council of Canada. ABA, IAA-Leu, IAA-Ala, IAA-Asp, IAA, zeatin (Z), zeatin-riboside (ZR), isopentenyladenosine riboside, and isopentenyladenosine were purchased from Sigma-Aldrich. dhZ and dhZR were purchased from Olchemim Ltd., and GA1, GA3, GA4, GA7, GA8, GA9,

GA19, GA20, GA24, GA29, GA44, and GA53 were purchased from the Research School of Chemistry, Australian National University. Deuterated forms of the hormones that were used as internal standards included d3-dihydroxyphaseic acid, d5-ABA-GE, d3-PA, d4-7′-OH-ABA, d3-neoPA, d4-ABA, d4-trans-ABA, d3-IAA-Leu, d3-IAA-Ala, d3-IAA-Asp, and d3-IAA-Glu, and they were synthesized and prepared at the National Research Council of Canada according to works by Abrams et al. (2003) and Zaharia et al. (2005). d5-IAA was purchased from Cambridge Isotope Laboratories. d3-dhZ, d3-dhZR, d5-Z-O-Glu, d6-iPR, and d6-iP were purchased from Olchemim Ltd. d2-GA1, d2-GA3, d2-GA4, d2-GA7, d2-GA8, d2-GA9, d2-GA19, d2-GA20, d2-GA24, d2-GA29, d2-GA34, d2-GA44, d2-GA51, and d2-GA53 were purchased from the Research School of Chemistry, Australian National University. Calibration curves were created for all compounds of interest. Quality control (QC) samples were run along with the tissue samples.

Instrumentation

Analysis was performed with ultraperformance liquid chromatography (UPLC)/electrospray ionization-mass spectrometry (MS)/MS using a Waters ACQUITY UPLC System equipped with a binary solvent delivery manager and a sample manager coupled to a Waters Micromass Quattro Premier XE Quadrupole Tandem Mass Spectrometer through a Z-spray interface. MassLynx and QuanLynx (Micromass) were used for data acquisition and data analysis.

Extraction and Purification

An aliquot (100 μL) containing all of the internal standards, each at a concentration of 0.2 ng μL^{-1}, was added to homogenized sample (approximately 50 mg); 3 mL of isopropanol:water:glacial acetic acid (80:19:1, v/v/v) was further added, and the samples were agitated in the dark for 14 to 16 h at 4°C. Samples were then centrifuged, and the supernatant was isolated and dried on a Büchi Syncore Polyvap. Furthermore, they were reconstituted in 100 μL of acidified methanol, adjusted to 1 mL with acidified water, and then, partitioned against 2 mL of hexane. After 30 min, the aqueous layer was isolated and dried as above. Dry samples were reconstituted in 800 μL of acidified methanol and adjusted to 1 mL with acidified water. The reconstituted samples were passed through equilibrated Sep-Pak C18 Cartridges (Waters Inc.), and the final eluate was split in two equal portions. One portion was dried completely (and stored), whereas the other portion was dried down to the aqueous phase on a LABCONCO Centrivap Concentrator (Labconco Corporation). The second portion was partitioned against ethyl acetate (2 mL) and further purified using an Oasis WAX Cartridge (Waters Inc.). The GA-enriched fraction in the second portion was eluted with 2 mL of acetonitrile:water (80:20, v/v) and then dried on a centrivap as described above. An internal standard blank was prepared with 100 μL of deuterated internal standards mixture. A QC standard was prepared by adding 100 μL of a mixture containing all of the analytes of interest, each at a concentration of 0.2 ng μL^{-1}, to 100 μL of internal standard mix. Finally, both portions, blanks, and QCs were reconstituted in a solution of 40% (v/v) methanol containing 0.5% (v/v) acetic acid and 0.1 ng μL^{-1} of each of the recovery standards.

Hormone Quantification by HPLC-ESI-MS/MS

Performed as a fee for service product by the National Research Council of Canada, samples were injected onto an ACQUITY UPLC HSS C18 SB Column (2.1 × 100 mm, 1.8 μm) with an inline filter and separated by a gradient elution of water containing 0.02% (v/v) formic acid against an increasing percentage of a mixture of acetonitrile:methanol (50:50, v/v). Briefly, the analysis uses the Multiple Reaction Monitoring function of the MassLynx v4.1 (Waters Inc.) control software. The resulting chromatographic traces are quantified offline by the QuanLynx v4.1 software (Waters Inc.), wherein each trace is integrated, and the resulting ratio of signals (nondeuterated to internal standard) is compared with a previously constructed calibration curve to yield the amount of analyte present (nanograms per sample). Calibration curves were generated from the Multiple Reaction Monitoring signals obtained from standard solutions based on the ratio of the chromatographic peak area for each analyte to that of the corresponding internal standard as described by Ross et al. (2004). The QC samples, internal standard blanks, and solvent blanks were also prepared and analyzed along each batch of tissue samples.

Pharmacological Inhibition of GA in the Wild Type

Two GAs inhibitors, CCC and DMZ, were exogenously applied to wild-type plant material at the concentrations of 0.2 and 0.4 mM. The two inhibitors were known to be targeting early and late metabolic positions of the GA biosynthesis, CCC and DMZ (Rademacher, 2000). Plantlets exposed to these inhibitors were harvested, freeze dried, ground up, subjected to cellulose estimation as previously described, and compared with control plantlets.

Chemical Complementation of *dwf1-1* Phenotypes with Exogenous GA

An F2 population (*dwf1-1* and the wild type) was used to select homozygous *dwf1-1* alongside the wild type. Each genotype was transferred to plates containing one-half-strength Murashige and Skoog medium supplemented with 5 μM GA_3 (Lo et al., 2008) and mock control plates. Plantlets were grown vertically with approximately four plants per plate (n = 10). The effect of GA_3 on expansion was evaluated visually by seedling length, and cellulose content was measured according to the work by Updegraff (1969).

RNA Extraction, Reverse Transcription-PCR, and Promoter Analyses

The pathway option of GRAMENE (www.gramene.org) was used to select candidate genes from the GA biosynthetic genes in *S. bicolor*. *Sorghum* sp. *CESA* genes were previously identified (Petti et al., 2013), and a list of target genes and primers was compiled (Supplemental Table S1). Total mRNA was extracted as per the work by Petti et al. (2013) and converted to single-strand complementary DNA (AB Applied Biosystem). Transcript abundance was quantified by SyBr Green semiquantitative assay and completed on each biological replicate (n = 3 biological and technical replicates) on a StepOne Real-Time System (AB Applied Biosystem). The ΔΔ method was used for quantifying the relative expression levels normalized against the actin gene (Supplemental Table S1). Promoters were defined as 4,000 bp upstream of the initiation codon and examined using the PLACE Database for cir-acting regulatory DNA elements (Higo et al., 1999).

Statistical Analyses

Statistical analysis used ANOVA, Student's t test, and Tukey's post hoc test. Analyses were carried out on Graphpad PRISM5. Significance was established at $\alpha = 0.05$.

Supplemental Data

The following supplemental materials are available.

Supplemental Figure S1. Transcriptional analysis of *Sorghum* sp. early GA biosynthetic genes.

Supplemental Figure S2. Analyses of auxins and cytokinins.

Supplemental Table S1. List of primers and sequences.

Supplemental Table S2. Promoter analyses data.

Received June 22, 2015; accepted July 18, 2015; published July 21, 2015.

LITERATURE CITED

Abrams SR, Nelson K, Ambrose SJ (2003) Deuterated abscisic acid analogs for mass spectrometry and metabolism studies. J Labelled Comp Radiopharm **46:** 273–283

Arioli T, Peng L, Betzner AS, Burn J, Wittke W, Herth W, Camilleri C, Höfte H, Plazinski J, Birch R, et al (1998) Molecular analysis of cellulose biosynthesis in Arabidopsis. Science **279:** 717–720

Asano K, Hirano K, Ueguchi-Tanaka M, Angeles-Shim RB, Komura T, Satoh H, Kitano H, Matsuoka M, Ashikari M (2009) Isolation and characterization of dominant dwarf mutants, Slr1-d, in rice. Mol Genet Genomics **281:** 223–231

Aya K, Ueguchi-Tanaka M, Kondo M, Hamada K, Yano K, Nishimura M, Matsuoka M (2009) Gibberellin modulates anther development in rice via the transcriptional regulation of *GAMYB*. Plant Cell **21:** 1453–1472

Bhattramakki D, Dong J, Chhabra AK, Hart GE (2000) An integrated SSR and RFLP linkage map of *Sorghum bicolor* (L.) Moench. Genome **43:** 988–1002

Billot C, Ramu P, Bouchet S, Chantereau J, Deu M, Gardes L, Noyer JL, Rami JF, Rivallan R, Li Y, et al (2013) Massive sorghum collection genotyped with SSR markers to enhance use of global genetic resources. PLoS One **8:** e59714

Bischoff V, Desprez T, Mouille G, Vernhettes S, Gonneau M, Höfte H (2011) Phytochrome regulation of cellulose synthesis in *Arabidopsis*. Curr Biol **21:** 1822–1827

Brown DM, Zeef LA, Ellis J, Goodacre R, Turner SR (2005) Identification of novel genes in *Arabidopsis* involved in secondary cell wall formation using expression profiling and reverse genetics. Plant Cell **17:** 2281–2295

Burke IC, Wilcut JW, Allen NS (2007) Viability and in vitro germination of Johnsongrass (*Sorghum halepense*) pollen. Weed Technol **21:** 23–29

Carpita NC, Gibeaut DM (1993) Structural models of primary cell walls in flowering plants: consistency of molecular structure with the physical properties of the walls during growth. Plant J **3:** 1–30

Chen PW, Chiang CM, Tseng TH, Yu SM (2006) Interaction between rice MYBGA and the gibberellin response element controls tissue-specific sugar sensitivity of alpha-amylase genes. Plant Cell **18:** 2326–2340

Chen S, Ehrhardt DW, Somerville CR (2010) Mutations of cellulose synthase (CESA1) phosphorylation sites modulate anisotropic cell expansion and bidirectional mobility of cellulose synthase. Proc Natl Acad Sci USA **107:** 17188–17193

Cheng H, Qin L, Lee S, Fu X, Richards DE, Cao D, Luo D, Harberd NP, Peng J (2004) Gibberellin regulates Arabidopsis floral development via suppression of DELLA protein function. Development **131:** 1055–1064

Cosgrove DJ, Jarvis MC (2012) Comparative structure and biomechanics of plant primary and secondary cell walls. Front Plant Sci **3:** 204

Daras G, Rigas S, Penning B, Milioni D, McCann MC, Carpita NC, Fasseas C, Hatzopoulos P (2009) The thanatos mutation in *Arabidopsis thaliana* cellulose synthase 3 (*AtCesA3*) has a dominant-negative effect on cellulose synthesis and plant growth. New Phytol **184:** 114–126

de Lucas M, Davière JM, Rodríguez-Falcón M, Pontin M, Iglesias-Pedraz JM, Lorrain S, Fankhauser C, Blázquez MA, Titarenko E, Prat S (2008) A molecular framework for light and gibberellin control of cell elongation. Nature **451:** 480–484

Desprez T, Juraniec M, Crowell EF, Jouy H, Pochylova Z, Parcy F, Höfte H, Gonneau M, Vernhettes S (2007) Organization of cellulose synthase complexes involved in primary cell wall synthesis in *Arabidopsis thaliana*. Proc Natl Acad Sci USA **104:** 15572–15577

Desprez T, Vernhettes S, Fagard M, Refrégier G, Desnos T, Aletti E, Py N, Pelletier S, Höfte H (2002) Resistance against herbicide isoxaben and cellulose deficiency caused by distinct mutations in same cellulose synthase isoform *CESA6*. Plant Physiol **128:** 482–490

Downes BP, Crowell DN (1998) Cytokinin regulates the expression of a soybean beta-expansin gene by a post-transcriptional mechanism. Plant Mol Biol **37:** 437–444

Fagard M, Desnos T, Desprez T, Goubet F, Refregier G, Mouille G, McCann M, Rayon C, Vernhettes S, Höfte H (2000) *PROCUSTE1* encodes a cellulose synthase required for normal cell elongation specifically in roots and dark-grown hypocotyls of *Arabidopsis*. Plant Cell **12:** 2409–2424

Frigerio M, Alabadí D, Pérez-Gómez J, García-Cárcel L, Phillips AL, Hedden P, Blázquez MA (2006) Transcriptional regulation of gibberellin metabolism genes by auxin signaling in Arabidopsis. Plant Physiol **142:** 553–563

Fukaki H, Tameda S, Masuda H, Tasaka M (2002) Lateral root formation is blocked by a gain-of-function mutation in the SOLITARY-ROOT/IAA14 gene of Arabidopsis. Plant J **29:** 153–168

Gonneau M, Desprez T, Guillot A, Vernhettes S, Höfte H (2014) Catalytic subunit stoichiometry within the cellulose synthase complex. Plant Physiol **166:** 1709–1712

Haruta M, Sabat G, Stecker K, Minkoff BB, Sussman MR (2014) A peptide hormone and its receptor protein kinase regulate plant cell expansion. Science **343:** 408–411

Hedden P, Kamiya Y (1997) Gibberellin biosynthesis: enzymes, genes and their regulation. Annu Rev Plant Physiol Plant Mol Biol **48:** 431–460

Hedden P, Phillips AL (2000) Gibberellin metabolism: new insights revealed by the genes. Trends Plant Sci **5:** 523–530

Held MA, Penning B, Brandt AS, Kessans SA, Yong W, Scofield SR, Carpita NC (2008) Small-interfering RNAs from natural antisense transcripts derived from a cellulose synthase gene modulate cell wall biosynthesis in barley. Proc Natl Acad Sci USA **105:** 20534–20539

Higo K, Ugawa Y, Iwamoto M, Korenaga T (1999) Plant cis-acting regulatory DNA elements (PLACE) database: 1999. Nucleic Acids Res **27:** 297–300

Huang D, Wang S, Zhang B, Shang-Guan K, Shi Y, Zhang D, Liu X, Wu K, Fu X, Zhou Y (2015) A gibberellin-mediated DELLA-NAC signaling cascade regulates cellulose synthesis in rice. Plant Cell **27:** 1681–1696

Huq E, Quail PH (2002) PIF4, a phytochrome-interacting bHLH factor, functions as a negative regulator of phytochrome B signaling in *Arabidopsis*. EMBO J **21:** 2441–2450

Irie K, Hua C, Tun YT, Kikuchi F, Fujimaki H, Kikuchi F, Nagamine T (2008) Genetic analysis of sterility caused by anther indehiscence gene linked with a semidwarfing gene locus, sd1 in rice. J Agric Sci **53:** 69–74

Itoh H, Tatsumi T, Sakamoto T, Otomo K, Toyomasu T, Kitano H, Ashikari M, Ichihara S, Matsuoka M (2004) A rice semi-dwarf gene, Tan-Ginbozu (D35), encodes the gibberellin biosynthesis enzyme, ent-kaurene oxidase. Plant Mol Biol **54:** 533–547

Keyes GJ, Paolillo DJ, Sorrels ME (1989) The effects of dwarfing genes *Rht1* and *Rht2* on cellular dimensions and rate of leaf elongation in wheat. Ann Bot **64:** 683–690

Kong L, Dong J, Hart GE (2000) Characteristics, linkage-map positions, and allelic differentiation of *Sorghum bicolor* (L.) Moench DNA simple-sequence repeats (SSRs). Theor Appl Genet **101:** 438–448

Kong W, Jin H, Franks CD, Kim C, Bandopadhyay R, Rana MK, Auckland SA, Goff VH, Rainville LK, Burow GB, et al (2013) Genetic analysis of recombinant inbred lines for Sorghum bicolor × Sorghum propinquum. G3 (Bethesda) **3:** 101–108

Koornneef M, van der Veen JH (1980) Induction and analysis of gibberellin sensitive mutants in *Arabidopsis thaliana* (L.) heynh. Theor Appl Genet **58:** 257–263

Lane DR, Wiedemeier A, Peng L, Höfte H, Vernhettes S, Desprez T, Hocart CH, Birch RJ, Baskin TI, Burn JE, et al (2001) Temperature-sensitive alleles of RSW2 link the KORRIGAN endo-1,4-β-glucanase to cellulose synthesis and cytokinesis in Arabidopsis. Plant Physiol **126:** 278–288

Lansac AR, Sullivan CY, Johnson BE, Lee KW (1994) Viability and germination of the pollen of sorghum [Sorghum bicolor (L.) Moench]. Ann Bot (Lond) **74:** 27–33

Lee I, Foster KR, Morgan PW (1998) Effect of gibberellin biosynthesis inhibitors on native gibberellin content, growth and floral initiation in Sorghum bicolor. J Plant Growth Regul **17:** 185–195

Lei L, Li S, Gu Y (2012) Cellulose synthase interactive protein 1 (CSI1) mediates the intimate relationship between cellulose microfibrils and cortical microtubules. Plant Signal Behav **7:** 714–718

Liu G, Godwin ID (2012) Highly efficient sorghum transformation. Plant Cell Rep **31:** 999–1007

Lo SF, Yang SY, Chen KT, Hsing YI, Zeevaart JAD, Chen LJ, Yu SM (2008) A novel class of gibberellin 2-oxidases control semidwarfism, tillering, and root development in rice. Plant Cell **20:** 2603–2618

Mace ES, Tai S, Gilding EK, Li Y, Prentis PJ, Bian L, Campbell BC, Hu W, Innes DJ, Han X, et al (2013) Whole-genome sequencing reveals untapped genetic potential in Africa's indigenous cereal crop sorghum. Nat Commun **4:** 2320

Menz MA, Klein RR, Mullet JE, Obert JA, Unruh NC, Klein PE (2002) A high-density genetic map of Sorghum bicolor (L.) Moench based on 2926 AFLP, RFLP and SSR markers. Plant Mol Biol **48:** 483–499

Ogi Y, Kato H, Maruyama K, Kikuchi F (1993) The effects of culm length and other agronomic characters caused by semidwarfing genes at the sd-1 locus in rice. Jpn J Breeding **43:** 267–275

Okuno A, Hirano K, Asano K, Takase W, Masuda R, Morinaka Y, Ueguchi-Tanaka M, Kitano H, Matsuoka M (2014) New approach to increasing rice lodging resistance and biomass yield through the use of high gibberellin producing varieties. PLoS One **9:** e86870

Ordonio RL, Ito Y, Hatakeyama A, Ohmae-Shinohara K, Kasuga S, Tokunaga T, Mizuno H, Kitano H, Matsuoka M, Sazuka T (June 13, 2014) Gibberellin deficiency pleiotropically induces culm bending in sorghum: an insight into sorghum semi-dwarf breeding. Sci Rep http://dx.doi.org/10.1038/srep05287

Paque S, Mouille G, Grandont L, Alabadí D, Gaertner C, Goyallon A, Muller P, Primard-Brisset C, Sormani R, Blázquez MA, et al (2014) AUXIN BINDING PROTEIN1 links cell wall remodeling, auxin signaling, and cell expansion in *Arabidopsis*. Plant Cell **26:** 280–295

Paterson AH (2008) Genomics of sorghum. Int J Plant Genomics **2008:** 362451

Paterson AH, Bowers JE, Bruggmann R, Dubchak I, Grimwood J, Gundlach H, Haberer G, Hellsten U, Mitros T, Poliakov A, et al (2009) The *Sorghum bicolor* genome and the diversification of grasses. Nature **457:** 551–556

Persson S, Paredez A, Carroll A, Palsdottir H, Doblin M, Poindexter P, Khitrov N, Auer M, Somerville CR (2007) Genetic evidence for three unique components in primary cell-wall cellulose synthase complexes in Arabidopsis. Proc Natl Acad Sci USA **104:** 15566–15571

Persson S, Wei H, Milne J, Page GP, Somerville CR (2005) Identification of genes required for cellulose synthesis by regression analysis of public microarray data sets. Proc Natl Acad Sci USA **102:** 8633–8638

Peterson R, Slovin JP, Chen C (2010) A simplified method for differential staining of aborted and non-aborted pollen grains. Int J Plant Biol **1:** e13

Petti C, Shearer A, Tateno M, Ruwaya M, Nokes S, Brutnell T, Debolt S (2013) Comparative feedstock analysis in Setaria viridis L. as a model for C4 bioenergy grasses and Panicoid crop species. Front Plant Sci **4:** 181

Plackett AR, Powers SJ, Fernandez-Garcia N, Urbanova T, Takebayashi Y, Seo M, Jikumaru Y, Benlloch R, Nilsson O, Ruiz-Rivero O, et al (2012) Analysis of the developmental roles of the *Arabidopsis* gibberellin 20-oxidases demonstrates that GA20ox1, -2, and -3 are the dominant paralogs. Plant Cell **24:** 941–960

Rademacher W (2000) Growth retardants: effects on gibberellin biosynthesis and other metabolic pathways. Annu Rev Plant Physiol Plant Mol Biol **51:** 501–531

Reiter WD, Chapple CC, Somerville CR (1993) Altered growth and cell walls in a fucose-deficient mutant of Arabidopsis. Science **261:** 1032–1035

Ross AR, Ambrose SJ, Cutler AJ, Feurtado JA, Kermode AR, Nelson K, Zhou R, Abrams SR (2004) Determination of endogenous and supplied deuterated abscisic acid in plant tissues by high-performance liquid chromatography-electrospray ionization tandem mass spectrometry with multiple reaction monitoring. Anal Biochem **329:** 324–333

Roudier F, Fernandez AG, Fujita M, Himmelspach R, Borner GHH, Schindelman G, Song S, Baskin TI, Dupree P, Wasteneys GO, et al (2005) COBRA, an *Arabidopsis* extracellular glycosyl-phosphatidyl inositol-anchored protein, specifically controls highly anisotropic expansion through its involvement in cellulose microfibril orientation. Plant Cell **17:** 1749–1763

Sasaki A, Ashikari M, Ueguchi-Tanaka M, Itoh H, Nishimura A, Swapan D, Ishiyama K, Saito T, Kobayashi M, Khush GS, et al (2002) Green revolution: a mutant gibberellin-synthesis gene in rice. Nature **416:** 701–702

Schmidhuber J, Tubiello FN (2007) Global food security under climate change. Proc Natl Acad Sci USA **104:** 19703–19708

Sethaphong L, Haigler CH, Kubicki JD, Zimmer J, Bonetta D, DeBolt S, Yingling YG (2013) Tertiary model of a plant cellulose synthase. Proc Natl Acad Sci USA **110:** 7512–7517

Taylor NG, Howells RM, Huttly AK, Vickers K, Turner SR (2003) Interactions among three distinct CesA proteins essential for cellulose synthesis. Proc Natl Acad Sci USA **100:** 1450–1455

Tsekos I (1999) The sites of cellulose synthesis in algae: diversity and evolution of cellulose-synthesizing enzyme complexes. J Phycol **35:** 635–655

Tuinstra MR, Wedel J (2000) Estimation of pollen viability in grain sorghum contribution no. 99-212-J from the Kansas Agric. Exp. Stn. Crop Sci **40:** 968–970

Ueguchi-Tanaka M, Nakajima M, Katoh E, Ohmiya H, Asano K, Saji S, Hongyu X, Ashikari M, Kitano H, Yamaguchi I, et al (2007) Molecular interactions of a soluble gibberellin receptor, GID1, with a rice DELLA protein, SLR1, and gibberellin. Plant Cell **19:** 2140–2155

Updegraff DM (1969) Semimicro determination of cellulose in biological materials. Anal Biochem **32:** 420–424

Wolf S, Hématy K, Höfte H (2012) Growth control and cell wall signaling in plants. Annu Rev Plant Biol **63:** 381–407

Xia B, Hanada K, Kikuchi F (1991) Character expression of the semidwarfing gene sd-1 in rice (Oryza sativa L.): 1. Effects of nitrogen levels on the expression of some agronomic characteristics. Jpn J Crop Sci **60:** 36–41

Xie L, Yang C, Wang X (2011) Brassinosteroids can regulate cellulose biosynthesis by controlling the expression of *CESA* genes in Arabidopsis. J Exp Bot **62:** 4495–4506

Xu YL, Li L, Wu K, Peeters AJ, Gage DA, Zeevaart JA (1995) The GA5 locus of *Arabidopsis thaliana* encodes a multifunctional gibberellin 20-oxidase: molecular cloning and functional expression. Proc Natl Acad Sci USA **92:** 6640–6644

Yamaguchi M, Ohtani M, Mitsuda N, Kubo M, Ohme-Takagi M, Fukuda H, Demura T (2010) VND-INTERACTING2, a NAC domain transcription factor, negatively regulates xylem vessel formation in *Arabidopsis*. Plant Cell **22:** 1249–1263

Zaharia LI, Galka MM, Ambrose SJ, Abrams SR (2005) Preparation of deuterated abscisic acid metabolites for use in mass spectrometry and feeding studies. J Labelled Comp Radiopharm **48:** 435–445